

**CHARACTERISATION OF NOVEL
MAGNETOCALORIC MATERIALS (MnCoGe)
FOR MAGNETIC REFRIGERATION
APPLICATION**

ABDUL RASHID ABDUL RAHMAN

**DOCTOR OF PHILOSOPHY
(ELECTRICAL AND ELECTRONICS
ENGINEERING)**

**UNIVERSITI PERTAHANAN NASIONAL
MALAYSIA**

2023

**CHARACTERISATION OF NOVEL MAGNETOCALORIC MATERIALS
(MnCoGe) FOR MAGNETIC REFRIGERATION APPLICATION**

ABDUL RASHID ABDUL RAHMAN

Thesis submitted to the Centre for Graduate Studies, Universiti Pertahanan Nasional
Malaysia, in fulfilment of the requirements for the Degree of Doctor of Philosophy
(Electric and Electronics Engineering)

2023

ABSTRACT

Conventional vapour compressor-based refrigeration systems are less energy-efficient and harmful to the environment due to chlorofluorocarbon (CFC), which can deplete the ozone layer and contribute to global warming. Therefore, an alternative solution that is both energy-efficient and environmentally friendly is desirable. Studies on magnetocaloric materials (MCMs) with excellent properties are important to demonstrate their suitability and potential use in refrigeration. This work has focus on MnCoGe-based compound for magnetic cooling, which does not contain high-cost rare earth elements and can provide a favourable working temperature range near room temperature. MnCoGe has unique properties where it exhibits two stable crystallographic structures which can manipulate the magneto-structural transition by adjusting the composition. The magnetic behaviour was analysed through its structural properties, magnetic measurement, and magnetic entropy change ($-\Delta S_M$) for $\text{MnCoGe}_{1-x}\text{Al}_x$ and $\text{MnCoGe}_{1-x}\text{Si}_x$. The neutron diffraction is employed to study the magnetic structure and the moment of material. This measurement focus on $\text{MnCoGe}_{0.97}\text{Al}_{0.03}$ only due to the Echidna and Wombat neutron beam instruments offer very limited beam time. The room temperature x-ray diffraction shows that the $\text{MnCoGe}_{1-x}\text{Al}_x$ ($x=0, 0.05, 0.1, 0.15$ and 0.2) alloys have a major phase consisting of TiNiSi-type structure for $x \leq 0.03$ and the Ni_2In -type structure for $x > 0.03$. For $\text{MnCoGe}_{1-x}\text{Si}_x$ ($x=0, 0.05, 0.1, 0.15$ and 0.2) alloys, the results indicate that the compounds have a major phase consisting of orthorhombic TiNiSi-type structure with increasing lattice parameter b and decreased others (a and c) with the increase of Si concentration. The $-\Delta S_M$ maximal value increased with the increase of Al content from

8.36 to 9.57 J·kg⁻¹K⁻¹ for $x = 0.00$ to 0.15. On the other hand, the MnCoGe_{1-x}Si_x compounds shows decreasing pattern from $-\Delta S_M \sim 8.36$ J kg⁻¹ K⁻¹ at $x=0$ to $-\Delta S_M \sim 5.49$ J kg⁻¹ K⁻¹ at $x=0.2$ with 5 T applied field. The theoretical study mainly focuses on the MnCoGe_{0.97}Al_{0.03} compound, as the compound shows that TiNiSi-type and Ni₂In-type structures start to coexist together which given the best interest to further study the nature of FM - PM transition. The obtained critical parameters concluded the compound having long-range ferromagnetic order, which is second-order type magnetic transition, thus, verified the experimental studies and confirmed the reliability of the compounds for magnetic refrigeration application.

ABSTRAK

Sistem penyejukan berasaskan pemampat wap konvensional kurang cekap tenaga dan berbahaya kepada alam sekitar disebabkan oleh klorofluorokarbon (CFC), yang boleh menipiskan lapisan ozon dan menyumbang kepada pemanasan global. Oleh itu, penyelesaian alternatif yang cekap tenaga dan mesra alam adalah wajar. Kajian tentang bahan magnetocaloric (MCM) dengan sifat yang sangat baik adalah penting untuk menunjukkan kesesuaian dan potensi penggunaannya dalam penyejukan. Kajian ini memberi tumpuan kepada sebatian berasaskan MnCoGe untuk magnet penyejukan, yang tidak mengandungi unsur nadir bumi yang berkos tinggi dan boleh memberikan julat suhu kerja yang baik berhampiran suhu bilik. MnCoGe mempunyai sifat unik di mana ia mempamerkan dua struktur kristalografi yang stabil dan boleh memanipulasi peralihan magneto-struktur. Kajian ini dianalisis melalui sifat strukturnya, pengukuran magnetik dan perubahan entropi magnetik ($-\Delta S_M$) untuk $\text{MnCoGe}_{1-x}\text{Al}_x$ dan $\text{MnCoGe}_{1-x}\text{Si}_x$. Difraksi neutron digunakan untuk mengkaji struktur magnet dan momen bahan. Pengukuran ini memfokuskan pada $\text{MnCoGe}_{0.97}\text{Al}_{0.03}$ sahaja kerana instrumen pancaran neutron Echidna dan Wombat menawarkan masa pancaran yang sangat terhad. Difraksi sinar-x menunjukkan bahawa aloi $\text{MnCoGe}_{1-x}\text{Al}_x$ ($x=0, 0.05, 0.1, 0.15$ dan 0.2) mempunyai fasa utama yang terdiri daripada struktur jenis TiNiSi untuk $x \leq 0.03$ dan struktur jenis Ni_2In untuk $x > 0.03$. Bagi aloi $\text{MnCoGe}_{1-x}\text{Si}_x$ ($x=0, 0.05, 0.1, 0.15$ dan 0.2), sebatian menunjukkan fasa utama yang terdiri daripada struktur jenis TiNiSi ortorombik dengan parameter kekisi b yang meningkat dan yang lain menurun (a dan c) dengan peningkatan Si. Nilai maksimum $-\Delta S_M$ meningkat dengan peningkatan kandungan Al daripada 8.36 kepada

9.57 J kg⁻¹K⁻¹ untuk $x = 0.00$ kepada 0.15. Sebaliknya, sebatian MnCoGe_{1-x}Si_x menunjukkan corak penurunan dari $-\Delta S_M \sim 8.36$ J kg⁻¹ K⁻¹ pada $x=0$ kepada $-\Delta S_M \sim 5.49$ J kg⁻¹ K⁻¹ pada $x=0.2$ dengan medan 5 T digunakan. Kajian teoretikal tertumpu kepada sebatian MnCoGe_{0.97}Al_{0.03}, kerana sebatian itu menunjukkan struktur jenis TiNiSi dan Ni₂In mula wujud bersama dan memberikan minat untuk mengkaji lebih lanjut sifat peralihan FM - PM. Parameter kritikal yang diperolehi menyimpulkan sebatian mempunyai susunan feromagnetik jarak jauh, iaitu peralihan magnet jenis tertib kedua, oleh itu, mengesahkan kajian eksperimen dan mengesahkan kebolehpercayaan sebatian untuk aplikasi penyejukan magnet.

ACKNOWLEDGEMENTS

My utmost gratitude goes to God, the most gracious, most merciful, for all the blessings that helped me cope throughout this study. I would like to give my most profound appreciation to my supervisor, Assoc. Prof. Dr. Muhamad Faiz Md Din, for his continuous support, time, and valuable discussions in this research. He has given endless efforts, guidance, ideas, and suggestions in assisting me to solve the problems encountered.

I am grateful to my co-supervisor, Assoc. Prof. Dr. Siti Nooraya Mohd Tawil for her invaluable advice and moral support. Also, to Assoc. Prof. Ts. Dr. Norinsan Kamil Othman from Universiti Kebangsaan Malaysia (UKM) for his technical support in assisting me with the experiment setup and sharing relevant knowledge and information. I would like to thank my research colleagues, Dr. Nur Sabrina Suhaimi and Dr. Nor Fazilah Mahamad Yusoff (UMT), for their technical support and knowledge sharing. Special thanks to the lab technicians for supporting the entire lab work on time. I thank my best friends, Dr. Muhamad Izzat Yusoff and Engr. Hafizuddin Jaafar, for their care, support, and faithful friendship. They kept my morals and spirit high throughout my studies.

I would like to thank the Majlis Amanah Rakyat (MARA) for providing the Graduate Excellent Programme scholarship. Also, thanks to the Universiti Pertahanan Nasional Malaysia (UPNM) for the technical research funding support.

Last and most importantly, I wish to express my deepest gratitude to my parents and grandparents, Abdul Rahman Ibrahim, Roziah Abu Bakar, Abu Bakar Berahim, and Allahyarhamah Saleha Majid, for their endless prayers, encouragement, and moral support. My special thanks to my siblings, Capt. Kamarul Ariffin, Capt. Nur Mysha Ravindran, Amirul Asyraf, Aqmar Haziq, Farah Wahidah and Muhammad Qayyum. Also, my cute nephew, Khoyr Ariffin and Ayyash Ariffin. Finally, I wish to thank all my families for always being there for me. Their constant prayers, thoughts, and support have provided me strength and courage to complete this research.

APPROVAL

The Examination Committee has met on **16 November 2022** to conduct the final examination of **Abdul Rashid Abdul Rahman** on his degree thesis entitled **Characterisation of Novel Magnetocaloric Materials (MnCoGe) For Magnetic Refrigeration Application.**

The committee recommends that the student be awarded the of Doctor of Philosophy (Electric and Electronics Engineering).

Members of the Examination Committee were as follows.

Prof. Dr. Mohd Taufik bin Ishak

Faculty of Engineering

Universiti Pertahanan Nasional Malaysia

(Chairman)

Dr. Khadijah binti Ismail

Faculty of Engineering

Universiti Pertahanan Nasional Malaysia

(Internal Examiner)

Assoc. Prof. Ir. Dr. Irni Hamiza Hamzah

Centre of Electrical Engineering Studies

Universiti Teknologi Mara Pulau Pinang

(External Examiner)

Prof. Dr. Ab Malik Marwan bin Ali

Faculty of Applied Science

Universiti Teknologi Mara Shah Alam

(External Examiner)

APPROVAL

This thesis was submitted to the Senate of Universiti Pertahanan Nasional Malaysia and has been accepted as fulfilment of the requirements for the degree of **Doctor of Philosophy (Electric and Electronics Engineering)**. The members of the Supervisory Committee were as follows.

Assoc. Prof. Dr. Muhamad Faiz Md Din

Faculty of Engineering

Universiti Pertahanan Nasional Malaysia

(Main Supervisor)

Assoc. Prof. Dr. Siti Nooraya Mohd Tawil

Faculty of Engineering

Universiti Pertahanan Nasional Malaysia

(Co-Supervisor)

Assoc. Prof. Ts. Dr. Norinsan Kamil Othman

Faculty of Science and Technology

Universiti Kebangsaan Malaysia

(Co-Supervisor)

UNIVERSITI PERTAHANAN NASIONAL MALAYSIA

DECLARATION OF THESIS

Student's full name : Abdul Rashid Abdul Rahman
Date of birth : 22 January 1991
Title : Characterisation of Novel Magnetocaloric Materials
(MnCoGe) For Magnetic Refrigeration Application
Academic session : 2018/2022

I hereby declare that the work in this thesis is my own except for quotations and summaries which have been duly acknowledged.

I further declare that this thesis is classified as:

CONFIDENTIAL (Contains confidential information under the official Secret Act 1972)*

RESTRICTED (Contains restricted information as specified by the organisation where research was done)*

OPEN ACCESS I agree that my thesis to be published as online open access (full text)

I acknowledge that Universiti Pertahanan Nasional Malaysia reserves the right as follows.

1. The thesis is the property of Universiti Pertahanan Nasional Malaysia.
2. The library of Universiti Pertahanan Nasional Malaysia has the right to make copies for the purpose of research only.
3. The library has the right to make copies of the thesis for academic exchange.

Signature

820811035607

IC/Passport No.

Date:

**Signature of Supervisor/Dean of CGS/
Chief Librarian

MUHAMAD FAIZ MD DIN

**Name of Supervisor/Dean of CGS/
Chief Librarian

Date:

*If the thesis is CONFIDENTIAL OR RESTRICTED, please attach the letter from the organisation with period and reasons for confidentiality and restriction.

** Witness

TABLE OF CONTENTS

	TITLE	PAGE
	ABSTRACT	ii
	ABSTRAK	iv
	ACKNOWLEDGEMENTS	vi
	APPROVAL	viii
	APPROVAL	ix
	DECLARATION OF THESIS	x
	TABLE OF CONTENTS	xi
	LIST OF TABLES	xiv
	LIST OF FIGURES	xv
	LIST OF ABBREVIATIONS	xix
	LIST OF SYMBOLS	xx
CHAPTER 1	INTRODUCTION	1
	1.1 Overview of Magnetic Refrigeration	2
	1.2 Problem Statement	5
	1.3 Research Objectives	6
	1.4 Scope and Limitations	8
	1.5 Organisation of Thesis	8
CHAPTER 2	LITERATURE REVIEW	10
	2.1 Background of MCE	11
	2.1.1 History and Important Milestones	11
	2.1.2 Thermodynamics of MCE	12
	2.1.3 Measurement of MCE	16
	2.2 Overview of Magnetocaloric Materials (MCM)	19
	2.2.1 Classification of Magnetic Transition	19
	2.2.2 Materials Exhibiting FOMT	21
	2.2.3 Materials Exhibiting SOMT	26
	2.2.4 Limitations of Past MCMs	28
	2.3 MnCoGe Based Magnetocaloric Alloys	29
	2.3.1 Structural and Martensitic Transformation	29
	2.3.2 Magnetic Properties and Magneto-structural Transition	31
	2.3.3 Enhance MCE-tailor Magneto-structural Transition	33
	2.3.4 Modifications in MnCoGe	34
	2.4 Thermodynamic Modelling of Magnetocaloric Transition	42
	2.4.1 Arrott Plots	42
	2.4.2 Landau Theory of Magnetic Transitions	43
	2.4.3 Critical Exponent Analysis	44
	2.5 Summary	46

CHAPTER 3	EXPERIMENTAL METHODOLOGY	47
	3.1 Overview of Experimental Methods	48
	3.2 Alloy Synthesis	49
	3.3 Characterisation and Measurement Techniques	50
	3.3.1 X-ray Diffraction	50
	3.3.2 Differential Scanning Calorimetry	52
	3.3.3 Neutron Diffraction	53
	3.3.4 Physical Property Measurement System (PPMS)	55
	3.3.5 Thermomechanical Testing	57
	3.4 Property Evaluation	57
	3.4.1 Structural Analysis	57
	3.4.2 MCE Property Evaluation	58
CHAPTER 4	STRUCTURAL, MAGNETIC PHASE TRANSITION AND MAGNETIC ENTROPY CHANGE OF MnCoGe_{1-x}Al_x MAGNETOCALORIC ALLOYS	60
	4.1 Introduction	61
	4.2 Structure Properties	62
	4.3 Magnetic Phase Transitions	65
	4.4 The Magnetocaloric Effect	67
	4.5 Neutron Diffraction	71
	4.6 Summary	75
CHAPTER 5	STRUCTURAL, MAGNETISM AND THERMOMECHANICAL PROPERTIES OF MnCoGe_{1-x}Si_x MAGNETOCALORIC ALLOYS	76
	5.1 Introduction	77
	5.2 Structure Properties	78
	5.3 Magnetic Phase Transitions	80
	5.4 The Magnetocaloric Effect	82
	5.5 Thermomechanical Testing	86
	5.6 Summary	89
CHAPTER 6	THEORETICAL MODELLING OF CRITICAL EXPONENTS ANALYSIS FOR MnCoGe_{0.97}Al_{0.03} COMPOUND	90
	6.1 Introduction	91
	6.2 Critical Behaviour of MnCoGe _{0.97} Al _{0.03} Compound	93
	6.2.1 Modified Arrott Plots	94
	6.2.2 Kouvel-Fisher Method	99
	6.2.3 Scaling Theory Method	103
	6.3 Summary	105
CHAPTER 7	CONCLUSION AND FUTURE RECOMMENDATION	106
	7.1 Conclusion	107
	7.2 Future Work	110

REFERENCES	112
BIODATA OF STUDENT	130
LIST OF PUBLICATIONS	131

LIST OF TABLES

TABLE NO.	TITLE	PAGE
Table 1.1	Comparison of current MCMs and MnCoGe based MCM	6
Table 2.1	Important milestones in MCE research	11
Table 2.2	Drawbacks and challenges in MCM	27
Table 2.3	The lattice parameters and atomic positions of MnCoGe at room temperature based on standard database in materialsproject.org	29
Table 2.4	The magnetic phase transitions, corresponding magnetic field changes $\mu_0\Delta H$, magnetic entropy change $-\Delta S_M$ and refrigeration capacities RC for the substitution for Mn in MnCoGe-based magnetocaloric alloys	34
Table 2.5	The magnetic phase transitions, corresponding magnetic field changes $\mu_0\Delta H$, magnetic entropy change $-\Delta S_M$ and refrigeration capacities RC for the substitution for Co in MnCoGe-based magnetocaloric alloys	36
Table 2.6	The magnetic phase transitions, corresponding magnetic field changes $\mu_0\Delta H$, magnetic entropy change $-\Delta S_M$ and refrigeration capacities RC for the substitution for Ge in MnCoGe-based magnetocaloric alloys	38
Table 2.7	The magnetic phase transitions, corresponding magnetic field changes $\mu_0\Delta H$, magnetic entropy change $-\Delta S_M$ and refrigeration capacities RC for the vacancies in MnCoGe-based magnetocaloric alloys.	40
Table 6.1	Derived critical exponents for MnCoGe _{0.97} Al _{0.03} with different theoretical models. Abbreviations: MAP = modified Arrott plot; KFM = Kouvel-Fisher method; WSR = Widom scaling relation	100

LIST OF FIGURES

FIGURE NO.	TITLE	PAGE
Figure 1.1	Comparison between gas compression and magnetic refrigeration cycles. The figure is adapted from.	3
Figure 2.1	The thermodynamic MCE cycle shows the variation in S_M with the temperature of the material.	12
Figure 2.2	Schematic of M vs T plot for MCM exhibiting (a) First-order magnetic transition and (b) Second-order magnetic transition.	19
Figure 2.3	The crystallographic unit cells of MnCoGe-based alloys (a) hexagonal Ni ₂ In-type structure (<i>P63/mmc</i> , austenitic phase) and (b) orthorhombic TiNiSi-type structure (<i>Pnma</i> , martensitic phase) based on database in materialsproject.org.	29
Figure 2.4	A schematic figure for the magnetic phase transitions, martensitic transformations and magneto structural transition between the orthorhombic (Orth) and hexagonal (Hex) phases for MnCoGe-based compounds based.	31
Figure 2.5	Arrott plots for La _{0.7} Pr _{0.3} Fe _{11.4-x} Cu _x Si _{1.6} (x = 0 and 0.06) compounds	42
Figure 3.1	Horizontal hierarchy representation of the experimental plan	47
Figure 3.2	Arc melting equipment used in the present work	49
Figure 3.3	Schematic of Bragg's law for constructive interference	50
Figure 3.4	Room temperature Rigaku MiniflexII XRD instrument operating at 40 kV, 30 mA with Cu K α radiation ($\lambda=1.5418$ Å) X-ray source.	51
Figure 3.5	(a) DSC Q100 (TA instruments) used for structural characterisation (b) DSC sample chamber containing the reference and the sample pan with heating module	52
Figure 3.6	Schematic diagrams of the (a) Echidna and (b) Wombat diffractometers	53

Figure 4.1	Measured $\text{MnCoGe}_{1-x}\text{Al}_x$ ($x = 0.03, 0.07, 0.1,$ and 0.15) powder XRD patterns at room temperature. The typical Ni_2In -type hexagonal (top) and TiNiSi -type orthorhombic (bottom) structures are denoted by the Miller indices hkl . The bottom sample is the refined pattern with $x = 0.15$ that includes the calculated, experimental, and different results.	62
Figure 4.2	M-T measured curves for $\text{MnCoGe}_{1-x}\text{Al}_x$ ($x = 0, 0.03, 0.07, 0.10, 0.15$ and 1.0) under the influence a magnetic field of 0.01 T.	63
Figure 4.3	DSC curves collected in the range of 250 - 500 K. The arrows indicate the structural transition and the Curies temperature.	64
Figure 4.4	Variation in magnetisation with an applied field of 0 - 5 T for the compounds (a) MnCoGe and (b) MnCoAl . The second-order transition Arott plots type for both compounds are shown in (c,d)	65
Figure 4.5	The isothermal magnetic entropy change, $-\Delta S_M(T, H)$ temperature dependence for $\text{MnCoGe}_{1-x}\text{Al}_x$ compounds ($x = 0, 0.03, 0.07, 0.1, 0.15,$ and 1.0) calculated from magnetisation isotherms with an applied field change of 0 - 5 T. Increasing fields are of the closed symbols while decreasing fields are of the open symbols.	67
Figure 4.6	The RC and $-\Delta S_M$ of $\text{MnCoGe}_{1-x}\text{Si}_x$ compounds for 0 - 5 T.	68
Figure 4.7	Neutron diffraction image for $\text{MnCoGe}_{0.97}\text{Al}_{0.03}$ collected at 6 - 450 K temperature range at 5 K steps over.	69
Figure 4.8	Neutron diffraction patterns for the $\text{MnCoGe}_{0.97}\text{Al}_{0.03}$ compound measured at 6 K, 300 K, 400 K, and 450 K. The pattern with symbols represent the experimental data, while the solid lines express calculated refinement data.	70
Figure 4.9	Temperature against the peak intensity for the $(002)^*$ and (011) peaks of the $\text{MnCoGe}_{0.97}\text{Al}_{0.03}$ compound.	71

Figure 4.10	Temperature function in terms of lattice parameters and unit cell volume of $\text{MnCoGe}_{0.97}\text{Al}_{0.03}$. denote the orthorhombic phase is denoted by open symbols with dots on the centre, denote the hexagonal phase is denoted by open symbols, and the corresponding phases in the mixed phase region is denoted by half-filled symbols.	72
Figure 5.1	(a) Refined XRD pattern of $\text{MnCoGe}_{1-x}\text{Si}_x$ ($x = 0.05, 0.10, 0.15,$ and 0.20) measured at room temperature. The refinement pattern includes the experimental and calculated results, and their difference is presented. (b) The inset shows the patterns for the indicated range of the $\text{MnCoGe}_{1-x}\text{Si}_x$ samples, demonstrating that the Bragg peaks shift to higher angles. (c) Rietveld refinement analysis indicating the lattice parameters and unit cell volumes.	77
Figure 5.2	M-T curves measured for $\text{MnCoGe}_{1-x}\text{Si}_x$ ($x = 0.05, 0.1, 0.15,$ and 0.2). The inset shows the pattern so Curie temperature with an increased Si concentration.	79
Figure 5.3	DSC curves collected in the range of 300-500 K with the arrows indicating the structural transition and Curie temperature.	80
Figure 5.4	Variation in magnetisation with an applied field of 0-5 T for the compounds of (a) $\text{MnCoGe}_{0.95}\text{Si}_{0.05}$ and (b) $\text{MnCoGe}_{0.85}\text{Si}_{0.15}$. The second-order transition Arrott plots type for both compounds are shown in (c,d).	81
Figure 5.5	Temperature dependence of the isothermal magnetic entropy change, $-\Delta S_M(T, H)$ for $\text{MnCoGe}_{1-x}\text{Si}_x$ compounds ($x = 0, 0.05, 0.10, 0.15, 0.20$) calculated from magnetisation isotherms with 0-5 T field change applied. Increasing fields is denoted by closed symbols while decreasing fields is denoted by open symbols.	83
Figure 5.6	The RC and $-\Delta S_M$ of $\text{MnCoGe}_{1-x}\text{Si}_x$ compounds for 0-5 T	84
Figure 5.7	Storage modulus (E') and Loss modulus (E'') measured for $\text{MnCoGe}_{1-x}\text{Si}_x$ ($x = 0, 0.05, 0.1, 0.15,$ and 0.2)	85
Figure 5.8	Tandelta measured for $\text{MnCoGe}_{1-x}\text{Si}_x$ ($x = 0, 0.05, 0.1, 0.15,$ and 0.2)	86

Figure 6.1	MnCoGe _{0.97} Al _{0.03} compound Isothermal magnetisation curves in the T_C vicinity.	91
Figure 6.2	MnCoGe _{0.97} Al _{0.03} compound Arrott plots (M^2 vs B/M) at temperatures within the T_C area.	92
Figure 6.3	Modified Arrott plots (M^2 vs B/M) with different theoretical models: (a) mean field ($\beta = 0.50$, $\gamma = 1.0$), b) 3D-Heisenberg ($\beta = 0.365$, $\gamma = 1.336$), c) 3D-Ising ($\beta = 0.325$, $\gamma = 1.24$), and d) Tricritical mean-field ($\beta = 0.25$, $\gamma = 1.0$) for MnCoGe _{0.97} Al _{0.03} compound at temperatures within the T_C area.	93
Figure 6.4	Temperature variation of the relative slope RS ($RS \equiv S(T)/S(T_C)$) for MnCoGe _{0.97} Al _{0.03} compound in typical theoretical models	94
Figure 6.5	Temperature dependence of the spontaneous magnetisation $M_S(T, 0)$ and the inverse initial susceptibility $\chi_0^{-1}(T, 0)$	96
Figure 6.6	Modified Arrott plot: isotherms of $M^{1/\beta}$ vs. $(B/M)^{1/\gamma}$ with the fitted exponents $\beta = 0.429$ and $\gamma = 0.80$	96
Figure 6.7	Kouvel-Fisher plot for the spontaneous magnetisation $M_S(T)$ and the inverse initial susceptibility $\chi_0^{-1}(T)$. (Solid lines are fitted to Equations (3) and (4).)	98
Figure 6.8	Isothermal $M(H)$ plots along with the log-log scale at $T_C = 352$ K, the solid curves are the fitting following Eq. (6.3)	99
Figure 6.9	Modified Arrott plot: isotherms of $M^{1/\beta}$ vs. $(B/M)^{1/\gamma}$ with the calculated exponents $\beta = 0.44$ and $\gamma = 0.83$, the parallel lines are guides for eyes	100
Figure 6.10	Universal curves by the scaling plots below and above T_C values for the MnCoGe _{0.97} Al _{0.03} compound	102
Figure 7.1	Schematic of the Single thermomagnetic oscillator setup showing the thermomagnetic alloy (TMA) at (a) the heat load and (b) the heat sink position	109
Figure 7.2	The schematic setup of the Hybrid thermomagnetic oscillator (HTMO) showing the thermomagnetic alloy (TMA) at (a) the heat load and (b) the heat sink position. (c) Experimental setup of the HTMO	109

LIST OF ABBREVIATIONS

DSC	-	Differential scanning calorimetry
FM	-	Ferromagnetic
FOMT	-	First order magnetic transition
GMCE	-	Giant magnetocaloric effect
HTMO	-	Hybrid thermomagnetic oscillator
MCE	-	Magnetocaloric effect
MCM	-	Magnetocaloric material
PM	-	Paramagnetic
PPMS	-	Physical property measurement system
RC	-	Refrigeration capacity
SOMT	-	Second order magnetic transition
STMO	-	Single thermomagnetic oscillator
VSM	-	Vibrating sample magnetometry
XRD	-	X-Ray diffraction
CFC	-	Chlorofluorocarbon
FWHM	-	Full width at half maximum
HFC	-	Hydrofluorocarbon
HCFC	-	Hydrochlorofluorocarbon
ICSD	-	Inorganic Crystal Structure Database
IEA	-	International Energy Agency
LP	-	Lorentz and Polarization
MM'X	-	M, M' = transition metals, X = carbon or boron group elements)

LIST OF SYMBOLS

θ	-	Theta (Angle)
T	-	Temperature
T_C	-	Curie temperature
T_{str}	-	Structural transformation temperatures
$-\Delta S_M$	-	Magnetic entropy change
E'	-	Storage modulus
E''	-	Loss modulus
α	-	Alpha
β	-	Betha
δ	-	Delta
γ	-	Gamma
M	-	Magnetic moment
B	-	Magnetic field
Mn	-	Manganese
Co	-	Cobalt
Ge	-	Germanium
Al	-	Aluminium
Si	-	Silicon
H	-	Hydrogen
S_M	-	Magnetic entropy
S_{lat}	-	Lattice entropy
T_{ad}	-	Adiabatic temperature
T_C^A	-	Austenite transition temperature
T_C^M	-	Martensite transition temperature
T_C^{orth}	-	Orthorhombic phase curie temperature
T_C^{hex}	-	Hexagonal phase curie temperature
T_M	-	Martensitic transformation
La	-	Lanthanum
Gd	-	Gadolinium

Fe	-	Iron
Cu	-	Copper
Ni	-	Nickel
Ga	-	Galium
C	-	Carbon
P	-	Steel group materials
Cr	-	Chromium
Zn	-	Zinc
E'	-	Elastic modulus
E''	-	Imaginary loss modulus
T _g	-	Glass transition temperature
V	-	Volume
V	-	Elements in Nitrogen group
R _{wp}	-	Weight residual
R _{bragg}	-	Bragg R factor

CHAPTER 1

INTRODUCTION

There is a rising demand for energy-efficient, environmentally sustainable materials and technologies in today's world. Because conventional refrigerators are harmful to the environment, magnetic refrigerators, which employ magnetocaloric materials' thermomagnetic response, have gained great demand due to their eco-friendly technology and energy-efficient cooling. This chapter provides an overview of magnetic refrigeration as well as the problem statement of this thesis, followed by the objective and organisation of this research.

1.1 Overview of Magnetic Refrigeration

Refrigeration systems used in commercial and residential buildings cooling contribute 700 million metric tons of CO₂ globally every year (~10% of all greenhouse gas emissions) and are responsible for nearly 15% of total energy consumption worldwide; total localized energy consumption in peak areas and at times can reach as high as 70% [1]. According to a 2018 report on cooling prepared by the International Energy Agency (IEA), only ~8% of the 2.8 billion residents own AC units in the world's hottest regions. This percentage will rise in tandem with their rapidly developing economies, resulting in a substantial increase in total energy consumption and CO₂ emissions [2]–[4]. Magnetic refrigerator (MR) provides an energy-efficient and environmentally friendly alternative to such conventional techniques as the conventional vapour compressor-based refrigerator uses harmful chlorofluorocarbons (CFCs) that can deplete the ozone layer and increases the rate of global warming [1], [3].

MR is a relatively novel technique that employs magnetically ordered materials and is based on the magnetocaloric effect (MCE), which results from the coupling of a system of magnetic moments with an external magnetic field resulting in the cooling or heating of a system. The critical phenomenon of a refrigeration system is a constriction of the degree of freedom, which increases the temperature. In the conventional gas compression (vapour cycle) refrigerator, the constriction is realised by a volume compression of the atom gas, whereas the magnetic refrigerator is realised by a constriction of the magnetic spins in magnetocaloric materials. Both magnetic and conventional vapour cycles are based on the four following steps, as illustrated in Figure 1.1. The first stage indicated the adiabatic compression or magnetisation, where

the temperature of the refrigerant increases due to the application of compression or the magnetic field. The second stage is iso-volume or iso-field cooling, where the surroundings extract the added heat. The third stage is the adiabatic expansion or demagnetisation, where the temperature of the refrigerant decreases due to an increased volume or the removal of the magnetic field. The last stage is iso-volume or iso-field heating, where the heat is loaded from the inside of the fridge.

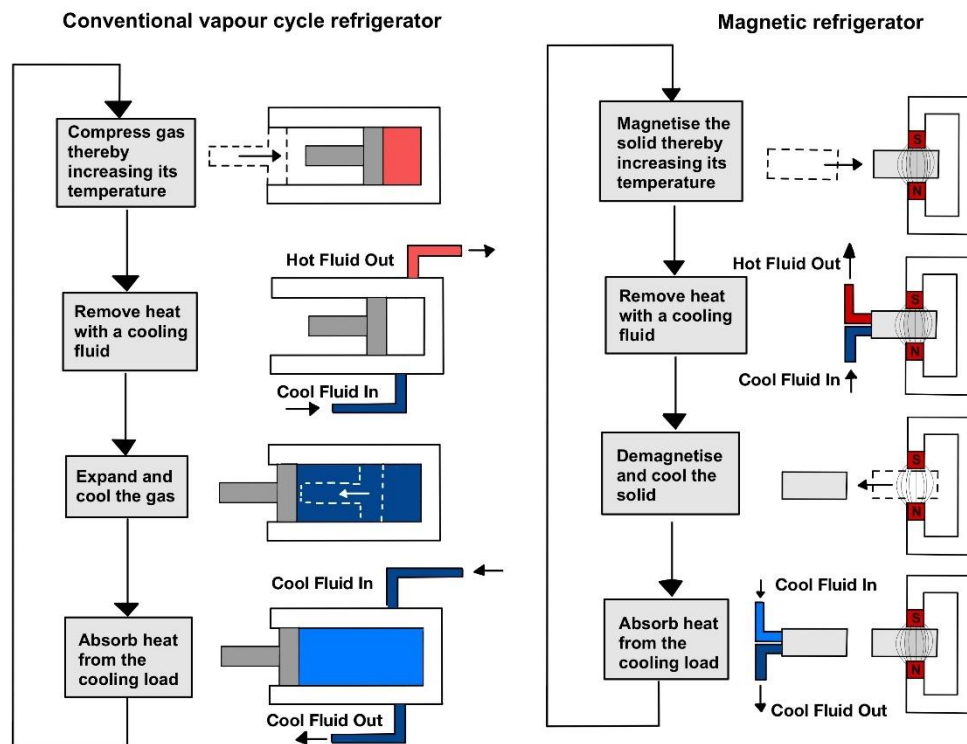


Figure 1.1 Comparison between gas compression and magnetic refrigeration cycles [5].

This magnetocaloric phenomenon was discovered in pure iron in 1881 by Emil Warburg [6]. A notable achievement in magnetic refrigeration was then made in 1976 by Brown, who proved magnetic refrigeration could work at ambient temperatures by generating a temperature difference of 47 K with a ferromagnetic refrigerant [7]. In 1997, there was a significant breakthrough at Ames laboratory/Astronautics Corporation of America with Profs. Karl A. Gschneider, Jr and V.K. Perchasky